

Ferromagnetic polarons in $\text{La}_{0.5}\text{Ca}_{0.5}\text{MnO}_3$ and $\text{La}_{0.33}\text{Ca}_{0.67}\text{MnO}_3$

G. Zheng and C.H. Patterson

*Department of Physics and Centre for Scientific Computation,
University of Dublin, Trinity College, Dublin 2, Ireland.*

(November 10, 2018)

Unrestricted Hartree-Fock calculations on $\text{La}_{1-x}\text{Ca}_x\text{MnO}_3$ ($x = 0.5$ and $x = 0.67$) in the full magnetic unit cell show that the magnetic ground states of these compounds consist of 'ferromagnetic molecules' or polarons ordered in herringbone patterns. Each polaron consists of either two or three Mn ions separated by O^- ions with a magnetic moment opposed to those of the Mn ions. Ferromagnetic coupling within the polarons is strong while coupling between them is relatively weak. Magnetic moments on the Mn ions range between 3.8 and $3.9 \mu_B$ in the $x = 0.5$ compound and moments on the O^- ions are $-0.7 \mu_B$. Each polaron has a net magnetic moment of $7.0 \mu_B$, in good agreement with recently reported magnetisation measurements from electron microscopy. The polaronic nature of the electronic structure reported here is obviously related to the Zener polaron model recently proposed for $\text{Pr}_{0.60}\text{Ca}_{0.40}\text{MnO}_3$ on the basis of neutron scattering data.

75.30.Et 75.47.Lx 71.27.+a 75.10.-b

I. INTRODUCTION

The current paradigm for the electronic structure of manganites ($\text{A}_{1-x}\text{B}_x\text{MnO}_3$) with $x \geq 1/2$ is a lattice of Mn sites with d^3 or d^4 orbital occupancy, with the proportion of each decided by the value of x and orbital ordering (OO) of the occupied e_g orbital on d^4 sites. The corresponding double-exchange model Hamiltonian has been studied extensively¹⁻³. Manganites with $x \geq 1/2$ usually exhibit a phase transition⁴⁻⁹ which has been assumed to be charge ordering (CO) of the d^3 and d^4 sites at a temperature well below the paramagnetic transition temperature. The conventional picture of the orbital and charge ordered phase with the CE magnetic structure¹⁰ is shown schematically in Fig. 1a.

The validity of this picture for the manganites has been questioned recently^{11,12}; its contradictions were pointed out by Goodenough in 1955¹³. An alternative picture, the Zener polaron¹⁴, which challenges the ideas of double-exchange and CO in the manganites, was recently proposed to account for the structure of $\text{Pr}_{0.60}\text{Ca}_{0.40}\text{MnO}_3$ determined by neutron scattering¹⁵. In the conventional CO and OO picture, ordering of the e_g electron on d^4 Mn sites is expected to induce a Jahn-Teller (JT) distortion; the long Mn-O bond distance in LaMnO_3 exceeds 2.15 \AA ^{10,16} while the Mn-O distance in cubic perovskite CaMnO_3 is 1.88 \AA ¹⁰. The lesser modulations of

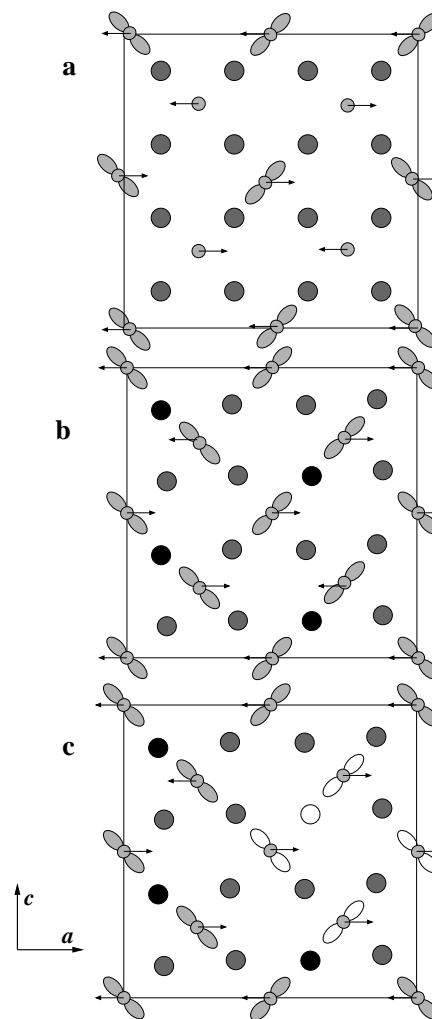


FIG. 1. Schematic illustrations of the magnetic unit cell for $\text{A}_{0.5}\text{B}_{0.5}\text{MnO}_3$ compounds with a CE magnetic structure: (a) the conventional double exchange picture; (b) the polaronic picture; (c) a possible change in orbital order in a small ferromagnetic domain when an electron is added at the oxygen ion site indicated by an unshaded circle. Spins are indicated by arrows, Mn d^4 sites by double-lobed orbitals, Mn d^3 sites by small shaded circles, O^{2-} ions by larger shaded circles and O^- ions by black circles.

bond length in doped manganites with $x \sim 1/2$ (1.92 and 2.06 \AA in $\text{La}_{0.5}\text{Ca}_{0.5}\text{MnO}_3$ ⁵ and 1.98 and 2.01 \AA in $\text{Pr}_{0.60}\text{Ca}_{0.40}\text{MnO}_3$ ¹⁵) suggest an intermediate valence.

In this Communication we report results of Unrestricted Hartree-Fock (UHF) calculations on $\text{La}_{1-x}\text{Ca}_x\text{MnO}_3$ for $x = 1/2$ and $x = 2/3$. The UHF electronic structure for these compounds is interpreted in terms of ferromagnetic polarons containing two ($x = 1/2$) or three ($x = 2/3$) Mn ions. The main difference between results from UHF calculations and the conventional double exchange picture is that all Mn ions are essentially d^4 . Consequently electrons must transfer from oxygen ions to every other Mn ion in the $x = 1/2$ compound, resulting in an ordered array of O^- ions between pairs of Mn ions. The structures of the polaron phases for $x = 1/2$ and $x = 2/3$ are shown schematically in Figs. 1b and 2.

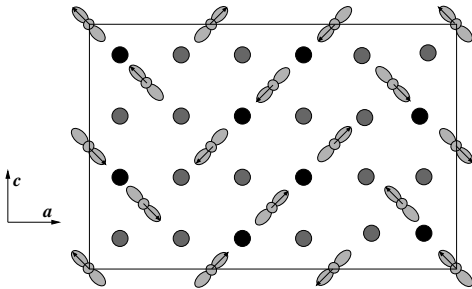


FIG. 2. Schematic illustration of the magnetic unit cell for $\text{La}_{0.33}\text{Ca}_{0.67}\text{MnO}_3$ with the experimentally observed magnetic structure. Spins are indicated by arrows, Mn d^4 sites by double-lobed orbitals, O^{2-} ions by shaded circles and O^- ions by black circles.

Mn-O^- -Mn and Mn-O^- -Mn- O^- -Mn chains constitute the polarons for $x = 1/2$ and $x = 2/3$, respectively. Mn magnetic moments are in the range 3.8 to $3.9 \mu_B$ for either compound while oxygen ions within the polarons have charges closer to O^- than O^{2-} and magnetic moments of $-0.7 \mu_B$. All other oxygen ions are essentially O^{2-} ions. Each polaron has a net magnetic moment of $7.0 \mu_B$, in good agreement with recently reported magnetisation measurements from electron holography and Fresnel imaging¹⁷.

UHF calculations predict that magnetic coupling within polarons is strong and ferromagnetic (FM) while coupling between polarons is much weaker and can be antiferromagnetic (AF) or FM; these observations lead to a natural explanation for the observed CE or A-type AF magnetic ground states of manganites with $x = 1/2$,⁸ and the magnetic ground state of $\text{La}_{0.33}\text{Ca}_{0.67}\text{MnO}_3$, which contains polarons with the magnetic moment roughly aligned along the polaron axis⁶. Given that the magnetic coupling within the polarons is strong and FM, the appropriate model Hamiltonian for these systems at low temperature is a Heisenberg Hamiltonian on a triangular lattice where each polaron is a single magnetic entity, rather than the conventional double exchange Hamiltonian.

Results of UHF our calculations are at odds with den-

sity functional theory (DFT) calculations in the local spin density approximation (LSDA) reported recently^{18,19} and with LSDA calculations done as part of this work using the same electronic structure code²⁰ in that UHF calculations predict a magnetic moment on oxygen ions within the polarons whereas DFT calculations do not.

II. UHF CALCULATIONS

All electron UHF calculations were performed for $\text{La}_{0.5}\text{Ca}_{0.5}\text{MnO}_3$ and $\text{La}_{0.33}\text{Ca}_{0.67}\text{MnO}_3$ using the low temperature structures refined using x-ray data by Radaelli and coworkers²¹ in the full (80 and 120 atom) magnetic unit cells.

Spin densities of $\text{La}_{0.5}\text{Ca}_{0.5}\text{MnO}_3$ (Fig. 3) and $\text{La}_{0.33}\text{Ca}_{0.67}\text{MnO}_3$ (Fig. 4) in the ac planes of the crystal structures clearly show the polaronic nature of the electronic structures, including the magnetic moment of the O^- ions opposed to those of the neighbouring Mn ions. The magnetic unit cells of either compound each contain four polarons in the ac planes shown.

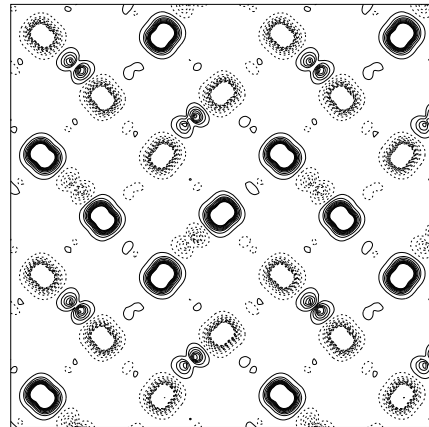


FIG. 3. UHF spin density plot for $\text{La}_{0.5}\text{Ca}_{0.5}\text{MnO}_3$ in the CE-AF state.

Magnetic moments and Mulliken populations on Mn and oxygen ions in the polarons are given in Table I.

Electron holography and Fresnel imaging¹⁷ measurements show that below the AF Néel temperature the $x = 1/2$ compound actually consists of both FM and AF domains and that the magnetic moment per Mn ion in the FM domains was $3.4 \pm 0.2 \mu_B$. UHF calculations predict a net magnetic moment of $7.0 \mu_B$ for the polaron, i.e. the polarons are fully spin polarised, in agreement with these measurements of the magnetisation of FM domains¹⁷. Earlier neutron scattering data for this compound (Table I) indicated magnetic moments somewhat smaller than these fully polarised values⁵ but the trend, where larger moments are found on the sites denoted Mn^{3+} , is reproduced.

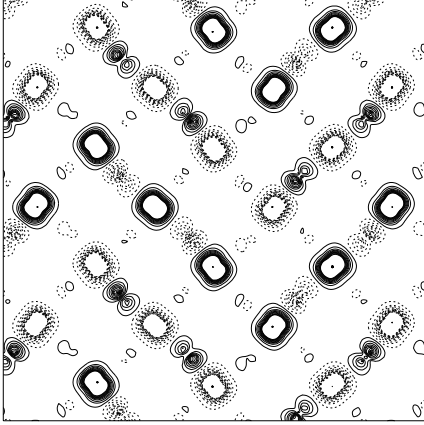


FIG. 4. UHF spin density plot for $\text{La}_{0.33}\text{Ca}_{0.67}\text{MnO}_3$ in AF state.

TABLE I. Charges and magnetic moments in $\text{La}_{0.5}\text{Ca}_{0.5}\text{MnO}_3$ from Mulliken populations and experiment.

	Mn moment μ_B	O moment μ_B
UHF (CE-AF) ^a	3.78, 3.91	-0.67
Expt. ^{ab}	2.57, 2.98	-
Expt. ^c	3.4 ± 0.2	-
	Mn charge	O charge
UHF (CE-AF) ^a	2.18, 2.17	-1.24

^aTwo values for the Mn moment are quoted as the Mn ions in the polaron are inequivalent

^bNeutron scattering, Ref.⁵

^cElectron holography, value obtained for FM domain per Mn ion, Ref.¹⁷

Mulliken populations from UHF calculations on $\text{La}_{1-x}\text{Ca}_x\text{MnO}_3$ indicate total Mn ion populations in the range 2.25 ($x = 0$) to 2.13 ($x = 1$) with a monotonic variation for intermediate values of x . Mn d populations have an even smaller relative variation across the range of x with a d population of 4.66 in LaMnO_3 , a range of d populations from 4.72 to 4.73 in $\text{La}_{0.5}\text{Ca}_{0.5}\text{MnO}_3$, and 4.70 in CaMnO_3 . This is consistent with a bonding picture in which the t_{2g} shell on each Mn ion is half-filled and a pair of e_g orbitals is combined with a set of four empty sp^3 orbitals to form a set of equivalent d^2sp^3 octahedral hybrid orbitals for polar-covalent Mn-O bonding. The consistency of both the Mn ion population and d population across the range of values of x contradicts the conventional double exchange picture where Mn ions are assumed to have their formal Mn^{3+} and Mn^{4+} charges.

Total energies were calculated for the FM state and four different low energy AF states of the $x = 1/2$ compound. Low energy states are found by flipping entire polaron magnetic moments; flipping the spin of one of the Mn ions in a polaron results in an increase of the total energy by around 400 meV. Energies of the various

low energy magnetic states of the $x = 1/2$ compound are well-fitted by an Ising-like, nearest-neighbour Hamiltonian of the form given in Eq. 1.

$$H = \sum_{\langle ij \rangle} J_{ij} \frac{\hat{S}_{zi} \cdot \hat{S}_{zj}}{S^2} \quad (1)$$

Labelling of exchange couplings is shown schematically in Fig. 5 and exchange constants obtained by fitting total energies of UHF calculations are given in Table II. The spin magnitude in Eq. 1 was chosen to be $S = 2$.



FIG. 5. Schematic illustration of exchange couplings between polarons in a Heisenberg Hamiltonian description.

Exchange couplings within the plane shown in Fig. 5 along zig-zag chains are FM and roughly equal in magnitude whereas they are AF perpendicular to the zig-zag chains. Exchange coupling between polarons in different planes is AF. The magnetic ground state is expected to be CE-type when J_{AF1} exceeds $(J_{FM1} + J_{FM2})/2$ in magnitude and A-type otherwise. Both are observed to be the magnetic ground state for various $x = 1/2$ compounds, depending on the A and B ion types⁸.

TABLE II. Exchange coupling constants derived from $\text{La}_{0.5}\text{Ca}_{0.5}\text{MnO}_3$ UHF calculations.

	Exchange constant (meV)
J_{AF1}	5
J_{AF2} ^a	8
J_{FM1}	-14
J_{FM2}	-12

^aAverage value over two interplanar couplings in crystallographic unit cell

Our calculations actually predict an A-type AF ground state whereas the CE-AF structure is the ground state in $\text{La}_{0.5}\text{Ca}_{0.5}\text{MnO}_3$ ¹⁰. However, in similar UHF calculations on LaMnO_3 ²², it was found that AF couplings are significantly underestimated compared to either experiment or results of configuration interaction (CI) cluster calculations, whereas FM couplings are in better agreement with both.

III. DISCUSSION

The polaronic picture for manganites with $x \geq 1/2$ which has been presented is consistent with a wide range

of experimental data and allows various observations, such as the unusual magnetisation in $\text{La}_{0.33}\text{Ca}_{0.67}\text{MnO}_3$, to be explained: it accounts for the observation of A-AF or CE-AF ground states for various combinations of counterion in $\text{A}_{0.5}\text{B}_{0.5}\text{MnO}_3$ ^{4,8}; it is consistent with full spin polarisation of Mn ions in $\text{La}_{0.5}\text{Ca}_{0.5}\text{MnO}_3$ ¹⁷.

One must be cautious in using UHF calculations to estimate magnitudes of magnetic moments on the oxygen ions. An analogy can be drawn between electron transfer from the O ion in a polaron to a neighbouring Mn ion and separation of the electron pair in a hydrogen molecule as the proton-proton distance is increased above the molecular equilibrium bond length: UHF wave functions for hydrogen molecules at large bond distances consist of a spin-up electron on one proton and a spin-down electron on the other; the additional configuration in which spins on protons have been exchanged is omitted, owing to the simple functional form of the wave function. UHF (and LSDA) wave functions incorporate strong electron correlation effects at the cost of a proper treatment of electron spin. Spin symmetry is restored in CI methods, but these can only be applied to finite clusters owing to the large number of electronic configurations encountered in that approach. CI calculations on the pair of MnO_6 octahedra in the polaron in $\text{La}_{0.5}\text{Ca}_{0.5}\text{MnO}_3$ show that the overall spin configuration is a linear combination of several determinants²³ with a magnetic moment on the central oxygen ion. The $\text{La}_{0.5}\text{Ca}_{0.5}\text{MnO}_3$ polaron electronic structure therefore resembles that in $\alpha\text{-NaV}_2\text{O}_5$ ²⁴; it is unlike the electronic structure which results in FM coupling in LaMnO_3 , which is very well described by a single spin configuration²².

An obvious question which arises within the polaron picture is, 'What happens when electrons are added to the $x = 1/2$ phase?' That is, 'What is the electronic structure predicted to be in the FM region of the phase diagram with $0.2 < x < 0.5$?' Since the bottom of the conduction band in $\text{La}_{0.5}\text{Ca}_{0.5}\text{MnO}_3$ is comprised largely of vacant oxygen 2p states on the O^- ion in the polaron, one would naturally expect to add the extra electron here. The spin density plots in Figs. 3 and 4 show that OO in the $x = 1/2$ compounds is *parallel* to the polaron axis, whereas it is T-shaped in LaMnO_3 (long Mn-O bonds in JT distorted octahedra in LaMnO_3 are *perpendicular* to each other). If the extra electron is added to the polaronic oxygen site, it is expected that there will be reorientation of e_g orbitals (Fig. 1c) and adjustment of Mn-O-Mn bond lengths. OO in the vicinity of the added electron is expected to resemble that in LaMnO_3 and one might expect to nucleate a small FM patch as further electrons are added.

ACKNOWLEDGMENTS

The authors wish to acknowledge discussions with W. Mackrodt, P.G. Radaelli, M. Towler, V. Ferrari and P.

Midgley. This work was supported by Enterprise Ireland under grant number SC/00/267.

-
- ¹ S. Yunoki, J. Hu, A. L. Malvezzi, A. Moreo, N. Furukawa and E. Dagotto, Phys. Rev. Lett. **80**, 845 (1998).
 - ² S. Fratini, D. Feinberg, and M. Grilli, cond-mat/0011419.
 - ³ E. Dagotto, T. Hotta, and A. Moreo, cond-mat/0012117.
 - ⁴ H. Kawano, R. Kajimoto, H. Yoshizawa, Y. Tomioka, H. Kuwahara and Y. Tokura, Phys. Rev. Lett. **78**, 4253 (1997).
 - ⁵ P. G. Radaelli, D. E. Cox, M. Marezio, S-W. Cheong, Phys. Rev. B **55**, 3015 (1997).
 - ⁶ P. G. Radaelli, D. E. Cox, L. Capogna, S-W. Cheong and M. Marezio, Phys. Rev. B **59**, 14440 (1999).
 - ⁷ K. H. Kim, M. Uehara and S-W. Cheong, cond-mat/0004467.
 - ⁸ R. Kajimoto, H. Yoshizawa, Y. Tomioka and Y. Tokura, Phys. Rev. B **66**, 180402 (2002).
 - ⁹ M. Pissas and G. Kallias, cond-mat/0205410.
 - ¹⁰ E. O. Wollan, W. C. Koehler, Phys. Rev. **100**, 545 (1955).
 - ¹¹ A. J. Millis, P. B. Littlewood, B. I. Shraiman, Phys. Rev. Lett. **74**, 5144 (1995).
 - ¹² G. M. Zhao, Phys. Rev. B **62**, 11639 (2000); G. M. Zhao, Y. S. Wang, D. J. Kang, W. Prellier, M. Rajeswari, H. Keller, T. Venkatesan, C. W. Chu, and R. L. Greene, Phys. Rev. B **62**, R11949 (2000)..
 - ¹³ J. B. Goodenough, Phys. Rev. **100**, 564 (1955).
 - ¹⁴ D. I. Khomskii and G. A. Sawatsky, Solid State Commun. **102**, 87 (1997).
 - ¹⁵ A. Daoud-Aladine, J. Rodriguez-Carvajal, L. Pinsard-Gaudart, M.T. Fernandez-Diaz, and A. Revcolevschi, Phys. Rev. Lett. **89**, 097205 (2002).
 - ¹⁶ J. Rodriguez-Carvajal, M. Hennion, F. Moussa, A.H. Moudden, L. Pinsard, A. Revcolevschi, Phys. Rev. B **57**, R3189 (1998).
 - ¹⁷ J. C. Loudon, N. D. Mathur, and P. A. Midgley, Nature, **420**, 797 (2002).
 - ¹⁸ Z. Popović and S. Satpathy, Phys. Rev. Lett. **88**, 197201 (2002).
 - ¹⁹ J.E. Medvedeva, V.I. Anisimov, O.N. Mryasov, and A.J. Freeman, cond-mat/0111038.
 - ²⁰ V.R. Saunders, R. Dovesi, C. Roetti, M. Causá, N. M. Harrison, R. Orlando, C. M. Zicovich-Wilson, Crystal98 User's Manual, University of Torino, Torino, 1998. (www.cse.dl.ac.uk/Activity/CRYSTAL)
 - ²¹ The P21/m structure used for $\text{La}_{0.5}\text{Ca}_{0.5}\text{MnO}_3$ was obtained by x-ray diffraction at 20 K (Table I Ref.⁵). The Pnma Wigner crystal structure used for $\text{La}_{0.33}\text{Ca}_{0.67}\text{MnO}_3$ was obtained by powder neutron diffraction at 1.5 K (Table V of Ref.⁶).
 - ²² M. Nicasastro and C. H. Patterson, Phys. Rev. B **65**, 205111 (2002).
 - ²³ C. H. Patterson (unpublished)
 - ²⁴ N. Suaud and M.-B. Lepetit, Phys. Rev. B **62**, 402 (2000).